Exact Distribution of Threshold Crossing Times for Protein Concentrations: Implication for Biological Timekeeping

Krishna Rijal[1,*] Ashok Prasad[2] Abhyudai Singh,[3] and Dibyendu Das[1,†]

[1]*Department of Physics, Indian Institute of Technology Bombay, Powai, Mumbai 400076, India*
[2]*Department of Chemical and Biological Engineering, Colorado State University, Fort Collins, Colorado 80523, USA*
[3]*Departments of Electrical and Computer Engineering, Biomedical Engineering and Mathematical Sciences, University of Delaware, Newark, Delaware 19716, USA*

Stochastic protein accumulation up to some concentration threshold sets the timing of many cellular physiological processes. Here we obtain the exact distribution of first threshold crossing times of protein concentration, in either Laplace or time domain, and its associated cumulants: mean, variance, and skewness. The distribution is asymmetric, and its skewness nonmonotonically varies with the threshold. We study lysis times of *E. coli* cells for holin gene mutants of bacteriophage-λ and find a good match with theory. Mutants requiring higher holin thresholds show more skewed lysis time distributions as predicted. The theory also predicts a linear relationship between infection delay time and host doubling time for lytic viruses, that has recently been experimentally observed.

Molecular biological processes associated with changes in cell state are controlled by changes in gene expression, a complex stochastic process involving transcription of a gene into a ribonucleic acid (RNA) molecule and its subsequent translation into a protein. Intrinsic noise in transcription and translation leads to a stochastically varying abundance of messenger RNA (mRNA) and proteins within cells, even when genetically identical [1–3]. Experimental studies have directly probed fluctuations of protein levels across cells [4,5]. Theoretical models assuming specific promoter configurations have solved for the coefficient of variance CV^2 (variance divided by square of mean) of the mRNA and protein numbers, as well as their full steady-state distributions [6–10]. Stochastic gene expression has been shown to be a fundamental property of living cells, affecting critical physiological processes of biological and biomedical importance [6,11].

The dynamics of downstream processes governed by the synthesis of a protein requires its accumulation to some minimum concentration threshold, e.g., transcription factors with sigmoidal Hill kinetics [12]. In such cases the timing of the downstream process is governed by the time at which the threshold concentration is reached for the first time, i.e., the First Passage Time (FPT) [13,14] of the stochastic gene expression process. The most well-studied example of timing control by stochastic protein accumulation is probably lysis of lambda phage-infected *E. coli*. Here the protein holin self-assembles on the bacterial membrane and punctures it after its concentration crosses a threshold, causing the cell to ultimately lyse or burst and release the newly formed viral particles [15,16]. The viral burst size of lambda phage-infected *E. coli* is known to

have a broad distribution [17]. While previous work has studied the timing of lysis and its relation with viral fitness [16,18,19] and the lysis-lysogeny decision [20], later studies have highlighted the distribution of lysis timing and demonstrated connections with the first passage time [21–24]. Fluctuations in lysis times lead to variations in viral burst sizes affecting both viral population fitness [25] as well as the health of the host. Genetic mutations of holin have been shown to regulate the stochasticity in lysis times in the λ variants [21,26,27].

First passage timing mechanisms based on protein accumulation may be quite common, from eukaryotic organisms to single cells. Recent work suggests that neuroblast migration timing in *C. elegans* development is controlled by the accumulation of *mig1* [28]. Cell division in *E. coli* has similarly been shown to be controlled by FtsZ expression [29]. Other examples include cell survival during prolonged drug exposure [30] and regulation of cell size in yeast cells by cdr2 proteins [31]. First passage times are also relevant for other phenomena such as RNA polymerase backtracking and cleavage [32], first binding of proteins to sites on DNA [33], capture of kinetochores [34], and more abstractly, estimating characteristics of energy landscapes [35]. Statistics of first passage times have been of great theoretical interest, and obtaining analytical expressions for their distribution (FPTD) is generally quite challenging [36]. In previous work we derived analytical expressions for the FPTD of the absolute number of any molecule generated through geometrically distributed burst kinetics to reach a threshold [37]. However, in living cells the cell volume is never constant, and for many biological processes the more appropriate

variable is not the absolute number but the concentration of proteins. For example, the variation of noise in lysis times of λ-phage mutants could be explained only assuming a concentration threshold of holins [27], and the concentration threshold of cdr2 proteins plays a role in the cell division of budding yeast [31].

Previously only approximate formulae existed for the moments of the concentration threshold crossing FPTD [23,27], and the distribution itself was unknown. Here we derive exact analytical expressions (as well as systematic approximations) for the FPTD of molecular concentrations and its moments, and apply them to experimental data on the distribution of lysis times. In the latter part of this text, we show that the threshold phenomenon can explain something out of the box: the experimentally seen linear relationship between mean lysis time and the doubling time of the host cell, after an infection.

A theoretical framework for the stochastic kinetics of protein synthesis has already been developed under the assumptions of short-lived mRNA and long-lived proteins. The exact steady-state distributions of the discrete protein number (n) has been derived previously [8] and was shown to follow a negative binomial distribution, while the continuous protein concentration $c = n/V$ (with V being cellular volume) was shown to follow the Gamma distribution [7,38]. While the *forward* continuous master equation was suitable to study the protein concentration c [7], the corresponding *backward* master equation [39] is more convenient for calculating the statistics of the FPT to reach the threshold concentration X. Given an initial $c = x < X$, the survival probability $S(X, x, t)$ that c survives reaching the threshold X through time t, satisfies the backward continuous master equation:

$$\frac{\partial S(X, x, t)}{\partial t} = k \int_x^X dx'[\nu(x' - x) - \delta(x' - x)]S(X, x', t) - \gamma x \frac{\partial S(X, x, t)}{\partial x}. \tag{1}$$

Here the initial condition is $S(X, x, 0) = 1$ and the boundary condition $S(X, x = X, t) = 0$; the rate of protein production $k\nu$ is assumed to be proportional to the mRNA production rate k and the experimentally known protein burst size distribution $\nu(x - x') = (1/b)e^{-(x-x')/b}$ with mean burst concentration b [5,38]. The rate of decay of the protein per unit concentration is γ which expresses the joint effect of protein degradation and cell growth. The FPTD for the *first* threshold crossing ($x \geq X$) in time t is obtained from $S(X, x, t)$ as $f(X, x, t) = -\partial S(X, x, t)/\partial t$. To solve Eq. (1) we convert the integro-differential equation into a partial differential equation and take the Laplace transform, $\tilde{S}(X, x, s) = \int_0^\infty dt e^{-st} S(X, x, t)$, leading to a differential equation for $\tilde{S}$ as a function of the (scaled) initial concentration $\tilde{x} = x/b$ (details in Sec. S2 of the Supplemental Material [40]):

$$\tilde{x}\frac{\partial^2 \tilde{S}(X, \tilde{x}, s)}{\partial \tilde{x}^2} + \left(\frac{k + \gamma + s}{\gamma} - \tilde{x}\right)\frac{\partial \tilde{S}(X, \tilde{x}, s)}{\partial \tilde{x}} - \frac{s}{\gamma}\tilde{S}(X, \tilde{x}, s) = -\frac{1}{\gamma}. \tag{2}$$

The homogeneous part of the above equation is a confluent hypergeometric equation [43]. Using the boundary condition and the fact that $\tilde{S}$ is finite as $x \to 0$, the solution in terms of the confluent hypergeometric function $_1F_1(a, c, \tilde{x})$ [43] is as follows (see Sec. S3 of the Supplemental Material [40]):

$$\tilde{S}(X, x, s) = \frac{1}{s}\left(1 - \frac{_1F_1[\frac{s}{\gamma}, 1 + \frac{k+s}{\gamma}, \frac{x}{b}]}{_1F_1[\frac{s}{\gamma}, 1 + \frac{k+s}{\gamma}, \frac{X}{b}]}\right). \tag{3}$$

Since $\tilde{f}(X, x, s) = 1 - s\tilde{S}(X, x, s)$, the desired exact FPTD in Laplace space for any γ and any initial protein concentration $x > 0$ is

$$\tilde{f}(X, x, s)|_{\gamma \neq 0} = \frac{_1F_1[\frac{s}{\gamma}, 1 + \frac{k+s}{\gamma}, \frac{x}{b}]}{_1F_1[\frac{s}{\gamma}, 1 + \frac{k+s}{\gamma}, \frac{X}{b}]}. \tag{4}$$

The above calculation (for $x > 0$) is applicable to the special case $x \to 0$ of interest, as the initial protein level is zero at the beginning of the translation. The case of exactly $x = 0$ requires a separate treatment, but is numerically identical to $x \to 0$ as expected (details in Sec. S3 of the Supplemental Material [40]).

For vanishing decay constant ($\gamma \to 0$), Eq. (4) simplifies to $\tilde{f}(X, x, s) = \exp\{-[(X - x)s/b(k + s)]\}$ which is analytically invertible and gives the exact FPTD in the time domain (see Sec. S4 of the Supplemental Material [40]):

$$f(X, x, t)|_{\gamma=0} = e^{-\frac{(X-x)}{b}}\left[e^{-kt}\sum_{n=1}^\infty \frac{(X-x)^n}{n!(n-1)!}\left(\frac{k}{b}\right)^n t^{n-1} + \delta(t)\right]. \tag{5}$$

Note that for $\gamma = 0$ the result is a function of the difference between the threshold and initial concentrations $(X - x)$, as expected from the translational symmetry in Eq. (1).

In general for $\gamma \neq 0$, Eq. (4) may be inverted numerically using *Mathematica* [44]. Finally we can also derive the exact expression of the first few moments, which are useful when comparing with empirical distributions. From Eq. (4), the nth moment $\langle t^n \rangle = [\partial^n \tilde{f}(X, x, s)/\partial s^n]|_{s\to 0}$. Defining $g(s) = {}_1F_1[(s/\gamma), 1 + \{(k + s)/\gamma\}, (x/b)]$, $h(s) = {}_1F_1[(s/\gamma), 1 + \{(k + s)/\gamma\}, (X/b)]$, $g^{(m)}(0) = [\partial^m g(s)/\partial s^m]|_{s\to 0}$ and $h^{(m)}(0) = [\partial^m h(s)/\partial s^m]|_{s\to 0}$, the first three moments are derived analytically exactly (see Sec. S5 of the Supplemental Material [40]):

$$\langle t \rangle = h^{(1)}(0) - g^{(1)}(0) \tag{6}$$

$$\langle t^2 \rangle = 2h^{(1)}(0)(h^{(1)}(0) - g^{(1)}(0)) + g^{(2)}(0) - h^{(2)}(0) \quad (7)$$

$$\langle t^3 \rangle = 6(h^{(1)}(0))^3 + g^{(1)}(0)(3h^{(2)}(0) - 6(h^{(1)}(0))^2)$$
$$+ 3h^{(1)}(0)(g^{(2)}(0) - 2h^{(2)}(0)) + h^{(3)}(0) - g^{(3)}(0). \quad (8)$$

Note that $\mathrm{CV}^2 = (\langle t^2 \rangle / \langle t \rangle^2) - 1$ and the skewness $= [(\langle t^3 \rangle - 3\langle t^2 \rangle \langle t \rangle + 2\langle t \rangle^3) / (\langle t^2 \rangle - \langle t \rangle^2)^{3/2}]$ follow from the above expressions.

Just like the distribution in Eq. (4), the quantities $g^{(1)}(0)$, $g^{(2)}(0)$, $g^{(3)}(0)$, $h^{(1)}(0)$, $h^{(2)}(0)$, and $h^{(3)}(0)$ (see Sec. S5 of the Supplemental Material [40]) depend on the four parameters (x/b), k, γ and (X/b).

Statistics of Lysis Times.—In order to match our results with experimental data, we used the raw data of Ref. [27]. Briefly, site-directed mutagenesis was used to generate a library of mutations in the S105 holin allele, each of which differed from the parent allele by one or two amino acid substitutions. These mutated sequences were then used to generate a library of lysogenic lambda phages, each carrying a slightly different holin gene. These viruses were used to infect *E. coli* cells, and lysis was thermally induced and measured at the single cell level for 91–174 cells per strain.

We estimate some required parameters as follows. Holins degrade slowly; hence the decay of x is mostly due to cell growth, with doubling time of roughly 40 min. Hence we choose $\gamma = \ln(2)/40 \ \mathrm{min}^{-1}$. We choose $x/b = 0.01$ to represent $x \to 0$, the vanishingly small initial protein concentration. Next we numerically eliminate the parameter (X/b) between the expressions of CV^2 and mean FPT $\langle t \rangle$ (see discussion in Sec. S7 in the Supplemental Material [40]), such that the theoretical curve of CV^2 versus $\langle t \rangle$ gets fixed by just one fitting parameter, i.e., k. The best fit of the theory to the experimental data for the 20 mutants is shown in Fig. 1, and yields the fitted value $k = 4.5 \ \mathrm{min}^{-1}$.
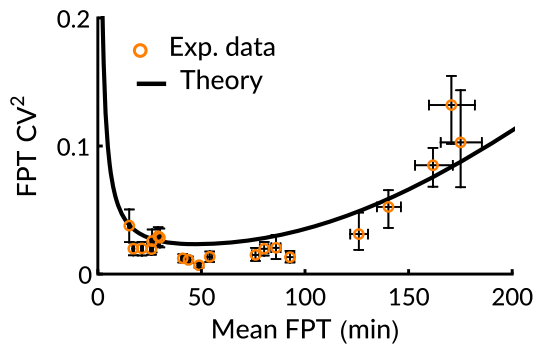

FIG. 1. CV^2 against $\langle t \rangle$ for 20 mutants (symbols) and exact theory (solid line) with best fit parameter $k = 4.5 \ \mathrm{min}^{-1}$. Error bars are 90% confidence intervals, obtained after bootstrapping 1000 replicates (see Sec. S6 of the Supplemental Material [40]). Here $\gamma = \ln(2)/40 \ \mathrm{min}^{-1}$ and $(x/b) = 0.01$.

The CV^2 curve has a minimum at mean FPT around $t_m \sim 40$ min.

While we expect the mutants to have roughly the same (x/b), k, and γ values (as given above), their mean FTP differs as does the threshold (X/b). We fix (X/b) for every mutant by matching the theoretical mean from Eq. (6) with the experimental average from the data, for that mutant. Then we obtain the full theoretical FPTD [by inverting Eq. (4) [44]] and plot against the experimental distribution to check how well they match. This is shown in Fig. 2 for two cases—mutant-1 (JD405) and mutant-2 (JD426) (see Sec. S1 of the Supplemental Material [40] and [27]) with the mean FPT smaller and larger than t_m respectively. See plots for the remaining 18 mutants in the Supplemental Material [40] (Fig. 3).

The data and theoretical curves (in Fig. 2) both suggest that FPTD is non-Gaussian and is skewed to the right. We explicitly study the variation of the skewness of FPTD for the mutants in Fig. 3—it shows a nonmonotonic behavior just like the CV^2 with a minimum around ~ 35 min close to t_m mentioned above. Thus mutants with increasingly larger mean FPT have increasingly asymmetric FPTD. Note that the distributions have asymptotic (large t) exponential tails $\sim \exp(-t/\tau_c)$, with characteristic times τ_c being related to the smallest pole $s_* = -1/\tau_c$ of $\tilde{f}(X, x, s)$ in Eq. (4). A plot of $\tau_c/\langle t \rangle$ against the mean FPT shows a similar nonmonotonic curve as CV^2 and skewness (see Sec. S8 in the Supplemental Material [40]).

Our results lead to an interesting prediction regarding the dependence of the mean lysis time on the cell doubling time. We showed above that fluctuations are minimal around a mean time t_m, for a given cellular size doubling time $\ln(2)/\gamma$. This value t_m for any bacterial cell however may vary, and depends upon experimental conditions which may change the cell doubling time. From the theory, we numerically calculate the t_m at minimum CV^2 and find it to be linearly dependent on the doubling time $\ln(2)/\gamma$ (see Fig. 4). We also show analytically that $t_m \approx -(1/\gamma)\ln(1 - f)$ where the fraction f is a ratio between an "optimal threshold" X_{opt} and the steady-state concentration $c_{\mathrm{ss}} = kb/\gamma$ (see Sec. S9 in the Supplemental

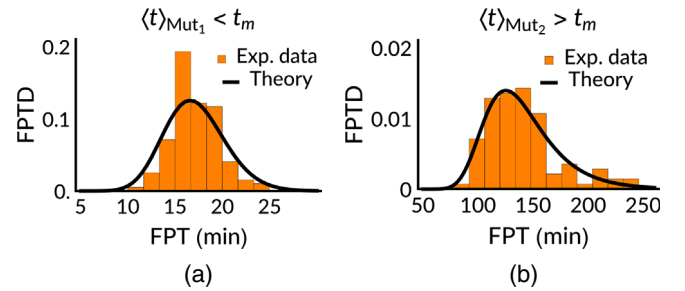FIG. 2. The FPTD from experiment and theory for (a) mutant-1 with $\langle t \rangle = 17.1$ min and (b) mutant-2 with $\langle t \rangle = 140.3$ min. Note $t_m \sim 40$ min.
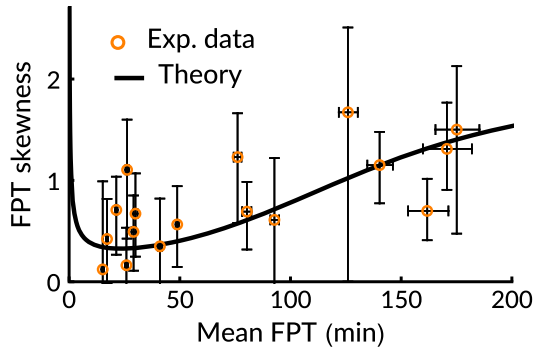
FIG. 3. Skewness against $\langle t \rangle$ for 20 mutants (symbols) and exact theory (solid line) with $k = 4.5$ min^{-1}, $x/b = 0.01$, and $\gamma = \ln(2)/40$ min^{-1}. Error bars are determined in a similar way as in Fig. 1.

Material [40]). Thus, under the plausible assumption that wild-type viruses have optimal noise characteristics, the mean lysis time of lambda phage under different host cell doubling times should be linearly related with cell doubling time. Interestingly, for a wide variety of viruses, a linear correlation between infection delay time and host doubling time has been reported recently [45].

Approximate FPTD.—Systematic approximations are useful since often they yield simpler expressions of practical use. Previous approximations for moments of the FPTD [23,27,46] were based on *ad hoc* assumptions. We develop a systematic approximate theory which matches the exact results up to second order in fluctuations as follows. Under the assumption that the burst sizes are small, the bursty term in Eq. (1) may be smoothed through the Kramers-Moyal expansion [39] (see Sec. S10 in the Supplemental Material [40]). Retaining terms up to second order, we obtain the following backward Fokker-Planck equation, valid for $x < kb/\gamma$:

$$\frac{\partial S(X,x,t)}{\partial t} = (kb - \gamma x)\frac{\partial S(X,x,t)}{\partial x} + kb^2\frac{\partial^2 S(X,x,t)}{\partial x^2}. \quad (9)$$
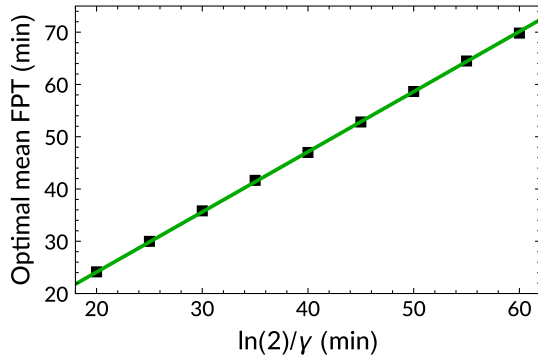

FIG. 4. Optimal mean FPT versus cell doubling time. As discussed in the text, the slope of the green line is equal to $-\ln(1-f)/\ln(2)$ with $f = 0.55$.

The forward Fokker-Planck equation (Sec. S10 in the Supplemental Material [40]) which is the counterpart of the above backward Eq. (9), is the corresponding Kramer-Moyal approximation to the exact theory developed in Ref. [7]. That forward equation, under Ito convention, is related to the following Langevin equation [39] (see Sec. S10 in the Supplemental Material [40] which includes Ref. [41]):

$$\frac{dc}{dt'} = kb - \gamma c + \eta(t') \quad (10)$$

where t' denotes the forward evolving time, and is to be distinguished from the "backward" time t. Note $\eta(t')$ is a Gaussian noise with $\langle \eta(t') \rangle = 0$ and $\langle \eta(t'_1)\eta(t'_2) \rangle = 2D\delta(t'_1 - t'_2)$, and the diffusion constant needs to be identified as $D = kb^2$. The simple Langevin equation with production, decay, and noise terms has appeared in earlier theories, e.g., of FPT for mRNA kinetics [47]—yet its exact FPTD was not known. We note that Eq. (9) corresponding to the Langevin Eq. (10), can be exactly solved to obtain the FPTD in Laplace space (see Sec. S11 in the Supplemental Material [40]):

$$\tilde{f}(X,x,s)|_{\gamma \neq 0}^{\text{approx}} = \frac{U\left[\frac{s}{2\gamma}, \frac{1}{2}, \frac{(bk - \gamma x)^2}{2b^2\gamma k}\right]}{U\left[\frac{s}{2\gamma}, \frac{1}{2}, \frac{(bk - \gamma X)^2}{2b^2\gamma k}\right]} \quad (11)$$

Here, U denotes Tricomi's confluent hypergeometric function related to $_1F_1$ (see Sec. S11 in the Supplemental Material [40]). From Eq. (11) the theoretical CV^2 and skewness may be obtained just as we did for the exact theory [Eq. (4)]—see Sec. S12 of the Supplemental Material [40] which includes Ref. [42].

The curves of CV^2 and skewness from the approximate FPTD [Eq. (11)] are plotted in Fig. 5 along with those from the exact theory [using Eqs. (7), (8)], and the ones from the Langevin simulations obtained using Eq. (10). The exact theory matches the approximate theory and simulations for CV^2 perfectly, but deviates a bit from those in the case of skewness, which is expected since in the Kramers-Moyal approximation we ignored third order moments which contribute to the skewness.

We derived analytically exact results for the FPTD for protein concentrations by solving the backward master equation. We showed that the FPTD and its moments match those observed for lysis times in lambda phage, reinforcing the hypothesis that the lysis time is governed by a protein accumulation-dependent FPTD. We developed a systematic approximation for the FPTD and derived analytical results for the approximate FPTD. The results are general and can be applied to fit lysis time distributions for all lytic phages including lambda phage, as well as other protein threshold crossing processes. The distributions themselves are non-Gaussian with exponential tails and may have a high
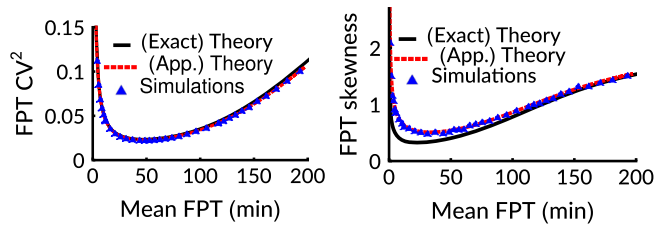
FIG. 5. The (a) CV^2 and (b) skewness, obtained from the exact continuous theory, the approximate theory, and the Langevin simulations are compared. The parameters are same as in Figs. (1) and (3).

skewness, indicating asymmetry that may be significant for some lytic phages. Our predictions may be checked using Gillespie simulations of protein numbers divided by time varying cellular volume [7] or using more exact time-dependent rates [48,49].

We showed that the FPT theory predicts that some mutants will have optimal noise characteristics, i.e., minimal CV and skewness, which is borne out by the data. The nonmonotonic relation between lysis time and noise suggests that lysis time may be selected during evolution to minimize noise, as suggested by the observation that the wild-type lambda phage has the lowest level of noise in lysis times [24].

We also predicted an interesting linear relationship between the optimal mean lysis time and the host cell doubling time. This result may be quite general for lytic viruses, since viral escape from an infected cell is typically characterized by a delay that could be a sign of a threshold phenomena. It is thus intriguing that for a wide variety of viruses, the initial burst timing is linearly correlated with the cell doubling time [45] across many different types of hosts and lysis times ranging from minutes to a week. Lytic phages are also important in phage therapy, where bacteriophages are used to kill pathogenic bacteria [50], and these results on lysis timing may have useful applications for that novel area of medicine.

*krishnarijal@iitb.ac.in
†dibyendu@phy.iitb.ac.in

[1] M. Thattai and A. Van Oudenaarden, Proc. Natl. Acad. Sci. U.S.A. **98**, 8614 (2001).
[2] M. B. Elowitz, A. J. Levine, E. D. Siggia, and P. S. Swain, Science **297**, 1183 (2002).
[3] J. M. Raser and E. K. O'shea, Science **309**, 2010 (2005).
[4] J. M. Raser and E. K. O'Shea, Science **304**, 1811 (2004).
[5] J. Yu, J. Xiao, X. Ren, K. Lao, and X. S. Xie, Science **311**, 1600 (2006).
[6] A. Sanchez, S. Choubey, and J. Kondev, Annu. Rev. Biophys. **42**, 469 (2013).
[7] N. Friedman, L. Cai, and X. S. Xie, Phys. Rev. Lett. **97**, 168302 (2006).
[8] V. Shahrezaei and P. S. Swain, Proc. Natl. Acad. Sci. U.S.A. **105**, 17256 (2008).
[9] A. Singh, C. A. Vargas, and R. Karmakar, in *Proceedings of the 52nd IEEE Conference on Decision and Control* (IEEE, New York, 2013), pp. 7217–7222.
[10] N. Kumar, A. Singh, and R. V. Kulkarni, PLoS Comput. Biol. **11**, e1004292 (2015).
[11] D. Fraser and M. Kaern, Mol. Microbiol. **71**, 1333 (2009).
[12] U. Alon, *An Introduction to Systems Biology* (CRC Press, Bristol, 2019).
[13] S. Redner, *A Guide to First-Passage Processes* (Cambridge University Press, Cambridge, England, 2001).
[14] G. Oshanin, R. Metzler, and S. Redner, *First-Passage Phenomena and Their Applications* (World Scientific Publishing Company, Singapore, 2014).
[15] U. Bläsi, P. Fraisl, C.-Y. Chang, N. Zhang, and R. Young, J. Bacteriol. **181**, 2922 (1999).
[16] R. White, S. Chiba, T. Pang, J. S. Dewey, C. G. Savva, A. Holzenburg, K. Pogliano, and R. Young, Proc. Natl. Acad. Sci. U.S.A. **108**, 798 (2011).
[17] M. Delbrück, J. Bacteriol. **50**, 131 (1945).
[18] I. N. Wang, D. L. Smith, and R. Young, Annu. Rev. Microbiol. **54**, 799 (2000).
[19] G. L. Ryan and A. D. Rutenberg, J. Bacteriol. **189**, 4749 (2007).
[20] M. G. Cortes, J. T. Trinh, L. Zeng, and G. Balázsi, Biophys. J. **113**, 2110 (2017).
[21] J. J. Dennehy and N. Wang, BMC Microbiol. **11**, 174 (2011).
[22] A. Singh and J. J. Dennehy, J. R. Soc. Interface **11**, 20140140 (2014).
[23] A. D. Co, M. C. Lagomarsino, M. Caselle, and M. Osella, Nucleic Acids Res. **45**, 1069 (2017).
[24] K. R. Ghusinga, J. J. Dennehy, and A. Singh, Proc. Natl. Acad. Sci. U.S.A. **114**, 693 (2017).
[25] I. N. Wang, Genetics **172**, 17 (2006).
[26] Y. Shao and I. N. Wang, Genetics **181**, 1467 (2009).
[27] S. Kannoly, T. Gao, S. Dey, N. Wang, A. Singh, and J. J. Dennehy, iScience **23**, 101186 (2020).
[28] S. Gupta, J. Varennes, H. C. Korswagen, and A. Mugler, PLoS Comput. Biol. **14**, e1006201 (2018).
[29] K. Sekar, R. Rusconi, J. T. Sauls, T. Fuhrer, E. Noor, J. Nguyen, V. I. Fernandez, M. F. Buffing, M. Berney, S. Jun et al., Mol. Syst. Biol. **14**, e8623 (2018).
[30] D. A. Charlebois, N. Abdennur, and M. Kaern, Phys. Rev. Lett. **107**, 218101 (2011).
[31] K. Z. Pan, T. E. Saunders, I. Flor-Parra, M. Howard, and F. Chang, eLife **3**, e02040 (2014).
[32] É. Roldán, A. Lisica, D. Sánchez-Taltavull, and S. W. Grill, Phys. Rev. E **93**, 062411 (2016).
[33] J. J. Parmar, D. Das, and R. Padinhateeri, Nucleic Acids Res. **44**, 1630 (2016).
[34] I. Nayak, D. Das, and A. Nandi, Phys. Rev. Research **2**, 013114 (2020).
[35] A. L. Thorneywork, J. Gladrow, Y. Qing, M. Rico-Pasto, F. Ritort, H. Bayley, A. B. Kolomeisky, and U. F. Keyser, Sci. Adv. **6**, eaaz4642 (2020).

[36] A. J. Bray, S. N. Majumdar, and G. Schehr, Adv. Phys. **62,** 225 (2013).

[37] K. Rijal, A. Prasad, and D. Das, Phys. Rev. E **102,** 052413 (2020).

[38] L. Cai, N. Friedman, and X. S. Xie, Nature (London) **440,** 358 (2006).

[39] C. W. Gardiner, *Handbook of Stochastic Methods* (Springer, Berlin, Berlin, 1985), Vol. 3.

[40] See Supplemental Material at http://link.aps.org/supplemental/10.1103/PhysRevLett.128.048101 for detailed calculations and experimental details, which includes Refs. [41] and [42].

[41] N. G. Van Kampen, J. Stat. Phys. **24,** 175 (1981).

[42] M. Abramowitz, I. A. Stegun, and R. H. Romer, *Handbook of Mathematical Functions with Formulas, Graphs, and Mathematical Tables* (Wolfram Library Archive, 1988).

[43] G. F. Simmons, *Differential Equations with Applications and Historical Notes* (CRC Press, Bristol, 2016).

[44] FixedTalbotNumericalLaplaceInversion.m, *Mathematica* online, version 12.2 (2003).

[45] T. Jin and J. Yin, Integr. Biol. **13,** 44 (2021).

[46] K. Biswas and A. Ghosh, Eur. Phys. J. E **44,** 16 (2021).

[47] M. Shreshtha, A. Surendran, and A. Ghosh, Phys. Biol. **13,** 036004 (2016).

[48] T. Lu, D. Volfson, L. Tsimring, and J. Hasty, Syst. Biol. **1,** 121 (2004).

[49] T. Carletti and A. Filisetti, Comput. Math. Methods Med. **2012,** 423627 (2012).

[50] S. T. Abedon, S. J. Kuhl, B. G. Blasdel, and E. M. Kutter, Bacteriophage **1,** 66 (2011).

Correction: A term was missing in Eq. (5) and has been inserted. A corresponding change has been made to the Supplemental Material.